

# SOFT HYDRATED SLIDING INTERFACES AS COMPLEX FLUIDS

BY

JHO KIM

THESIS

Submitted in partial fulfillment of the requirements  
for the degree of Master of Science in Mechanical Engineering  
in the Graduate College of the  
University of Illinois at Urbana-Champaign, 2016

Urbana, Illinois

Advisor:

Assistant Professor Alison C. Dunn

## ABSTRACT

Hydrogel surfaces are biomimics for sensing and mobility systems in the body such as the eyes and large joints due to their important characteristics of flexibility, permeability, and integrated aqueous component. Recent studies have shown polymer concentration gradients resulting in a less dense region in the top micrometers of the surface. Under shear, this gradient is hypothesized to drive lubrication behavior due to its rheological similarity to a semi-dilute polymer solution. In this work we map 3 lubricating regimes between a polyacrylamide surface and an aluminum annulus using stepped-velocity tribo-rheometry over 5 decades of sliding speed in increasing and decreasing steps. We postulate that the mechanisms of hydrogel-against-hard material lubrication are due to distinct complex fluid behavior characterized by weakly or strongly time-dependent response and thixotropy-like hysteresis. Tribo-rheometry is particularly suited to uncover the lubrication mechanisms of complex interfaces such as are formed with hydrated hydrogel surfaces and biological surfaces.

## ACKNOWLEDGMENTS

I would like to express sincere gratitude to my advisor Prof. Alison C. Dunn for her careful guidance and encouragement. This thesis could be completed with lots of advice and help from her.

Thank you to Prof. Randy Ewoldt for the kind use of his laboratory and his rheological expertise on this study, and to Jonathon Schuh for teaching me to use a rheometer and helping me to conduct every experiment of this study.

## TABLE OF CONTENTS

CHAPTER 1: INTRODUCTION.....	1
1.1 Background of oscillatory tribological measurements.....	2
1.2 Tribo-rheometry.....	3
1.3 Theories related to the research.....	4
1.3.1 Existing polymer physics basis for hydrogel lubrication.....	4
1.3.2 Thixotropy.....	6
1.4 Overview of the research.....	7
1.5 Figures.....	9
CHAPTER 2: MATERIALS AND METHODS.....	12
2.1 Experimental setup and materials.....	12
2.2 Experimental conditions.....	13
2.3 Figures.....	14
2.4 Tables.....	16
CHAPTER 3: RESULTS.....	17
3.1 Lubrication curves for soft hydrated interfaces.....	17
3.2 Lubrication hysteresis.....	19
3.3 Induced Normal Stress.....	19
3.4 Temperature inquiry.....	20
3.5 Figures.....	21

CHAPTER 4: DISCUSSION.....	24
4.1 Tribology of Soft Hydrated Interfaces.....	24
4.1.1 Friction Models.....	24
4.1.2 Surface stability under shear.....	27
4.1.3 Anchored Complex fluid lubrication.....	27
4.2 Conceptual complex soft interface lubrication.....	30
4.2.1 Lubrication regimes.....	30
4.2.2 Possible mechanisms for thixotropy-like lubrication.....	32
4.3 Figures.....	35
CHAPTER 5: CONCLUSION.....	38
REFERENCES.....	42
APPENDIX A.....	49

## CHAPTER 1: INTRODUCTION

Biological lubrication such as in the eye or at the cartilage of the knee relies on permeable membranes and solvated hydrophilic macromolecules such as mucins and lubricin. Hydrogels and solvated polymer brushes are increasingly used to study the slippery nature of these interfaces, and provide a controlled material and surface from which to begin connecting material properties to lubricating ability [1]–[6], as well as designing the next generation of cartilage scaffolds [7]–[11]. The lubricating performance of hydrogel surfaces and interfaces is dependent upon the composition, but also dependent upon the surface termination imparted by the method of cure and the mold material [12], [13]. Further, oxidation crosslinking and cure has resulted in a measurably less dense surface layer in poly(N,N-dimethylacrylamide) (PDMA) hydrogels as detected by shear rheology and neutron reflectivity, for *any* mold material [14]. In a sliding interface, a less dense surface layer will allow more mobility of polymeric species such as crosslinked chains, dangling loops, and dangling ends [15] (Figure 1.1). These possible sub-nanoscale features render the presenting hydrogel “surface” as integrated into the solvent rather than a clear boundary between solid and liquid phases. Surfaces with combined solid and fluid character present a challenge in understanding their lubrication mechanisms through traditional tribological

testing; therefore, new experimental approaches are needed to capture the fluid contribution to lubrication.

### 1.1 Background of oscillatory tribological measurements.

Soft matter surfaces often fare poorly in traditional tribological instruments due to their fragility, hydration, complex or curved geometry, and exceedingly low friction coefficients regularly reaching  $\mu < 0.01$  [16]–[18]. Recent micro-tribology instruments have overcome some of these challenges by substantial re-designs and moving away from strain-gage-based force transducers, which allows for low-pressure, local measurements [2], [19]–[22]. Reciprocating, or oscillatory, sliding motions are the most common because they require only small sample sizes and can attain many cycles in short times. However, the frequency of passing experienced by any contact location changes depending upon whether the stage is moving in forward or reverse. Because of this, the question of history-dependent lubrication may significantly affect the suitability of reciprocating migrating contact, especially when the passing frequency closely competes with other timescales of the surface material such as viscoelasticity.

## 1.2 Tribo-rheometry

An instrument capable of removing the oscillatory nature of tribological measurements while still prescribing constant-slip conditions under exceedingly low contact pressures is necessary to assess the complex rheological nature of the soft and hydrated interfaces. Traditional tribological instrumentation has been the “thrust washer bearing” experimental setup which measures the lubricating ability of a ring-on-flat for axial, or thrust loads. However, the high-precision normal force and torque requirements for low-pressure lubricity ( $\mu < 0.01$  at  $P < 5$  kPa) are already found in rheometers. Therefore, tribological study on rheometer, or tribo-rheometry, can be suitable method for soft, hydrated-surface tribology.

This tribo-rheometry testing has been conducted in various researches. In an effort to explicitly connect rheology and tribology, Kavehpour and McKinley generated “Stribeck” lubrication curves using a thrust-washer type annular ring rotating against a flat, as well as a more general gap-corrected friction map of effective viscosity versus shear rate [23], [24]. As the gap height was reduced to near the roughness of the parallel plates in the rheometer, the effective viscosity increased dramatically, indicating the boundary sliding regime. Thus a single experiment captured the lubrication transitions of various fluids between parallel rotating plates, co-designating the internal friction of a fluid, viscosity  $\eta$ , and the sliding friction,  $\mu$ , under a variety of loads, fluids, and gap heights. Also, JP Gong and



colleagues have studied hydrogel lubrication for the last 15 years by using a parallel-plate rheometer to first compress a hydrogel to known normal stress, then applying rotation at steps of increasing velocity and recording torque response. By conducting various pairs of hydrogel-solid surface experiments, they differentiated two cases of hydrogel friction, repulsive and adhesive cases, based on whether a hydrogel polymer chain is “repelled from or adsorbed on” solid counter-surface, and suggested a friction model named “repulsion-adsorption model.” [1]

### 1.3 Theories related to the research

#### 1.3.1 Existing polymer physics basis for hydrogel lubrication.

Attractive case of “repulsion-adsorption” model by Gong’s group shows two regimes associated with “elastic friction” and “hydrodynamic lubrication” (Figure 1.2) [1], [25]. The transition between the regimes is similar to the drop on the Stribeck curve as the resistance to sliding shifts from asperity contact to fluid shear. The thresholds of transition  $V^*$  (Eqn 1.3) are predicted to arise from single-chain polymer mechanics. They postulate that as the time to traverse one mesh size in a sliding experiment (Eqn 1.1) decreases past the relaxation time of a single polymer chain (Eqn 1.2), the lubricating mechanism changes from one lubrication to a second regime which engages the surface chains differently

because they do not have sufficient time to relax. In velocity under the relaxation velocity  $V^*$  (Eqn 1.3), “elastic friction” dominates the hydrogel friction, whose mechanism is based on rubber friction model by Schallamach.[26] If velocity increases beyond  $V^*$ , “hydrodynamic lubrication” becomes dominant, so friction increases monotonically in high velocity.

$$\tau = \xi/V \quad (\text{Eqn 1.1})$$

$$\tau^* = \frac{\xi^3 \eta}{k_B T} \quad (\text{Eqn 1.2})$$

$$V^* = \xi/\tau^* \quad (\text{Eqn 1.3})$$

Sawyer’s group found a similar transition point of lubrication in their study of hydrogel-hydrogel contact, which they named as “Gemini contact.”[2] In their “Gemini contact” friction study using high precision micro-tribometer in unidirection rotating sliding, they found two lubrication regimes named “Thermal fluctuation lubrication” and “Polymer relaxation lubrication.” (Figure 1.3) The transition between two regimes is predicted using polymer relaxation time as well.

The elegant trend in friction coefficient with mesh size is undeniable [16], but only to the extent that the mesh size of the bulk *subsurface* material can represent the morphology of the *surface*. It is known that both physical polymerization of polyvinyl alcohol (PVA) and redox free radical polymerization of poly(N,N-dimethylacrylamide) (PDMA) can produce detectable sub-micron surface layers

that are less stiff and less dense than the bulk, respectively [12]–[14]. In addition, any incomplete polymerization may create surface domains of more or less chain extension into solution [27]. Thus, open questions remain regarding the changes in surface regions with changes in mesh size, and subsequently the extent to which lubricating behavior is affected.

### 1.3.2 Thixotropy

One important concept dealt in this study is thixotropic behavior of complex fluid. Thixotropy is a phenomenon related to viscosity of a fluid, which decreases over time when shear is applied in the fluid.[28] This phenomenon is reversible, which means that shear-induced viscosity decrease can be recovered over time when amount of exerted shear decreases.

This change in viscosity results in a unique shape of shear stress response of thixotropic fluid to step changes in shear rate. (Figure 1.4 A-B) When step increase in shear rate occurs, shear stress jumps up at the beginning because the fluid has viscosity of previous step, but decreases over time because viscosity decreases over time. Similarly, when step decrease in shear rate is applied, shear stress shows undershoot followed by increase over time. This differs from simple shear thinning because the steady-state response takes time to emerge. It also differs from viscoelastic behavior where there is no torque overshoot, but a

monotonic approach of the torque to the steady-state value. In addition, bulk rheology of polyacrylamide hydrogels at similar polymer concentrations has shown that elasticity rather than viscoelasticity dominates their response[29], [30]. The expected stress response due to thixotropy-like sequential step increases and decreases of shear rate is described in Figure 1.4 C.

Complex behavior of thixotropic fluid can be explained in microscale using shear dependent behavior of particles inside the fluid. When there is no shear, particles gather together by weak bond to become larger flocs. If shear rate is applied, these flocs easily break over time into smaller flocs by action of flow, making the fluid easier to flow, or less viscous.

The characteristic of thixotropic complex fluid is used to explain experimental results of this study in CHAPTER 4: DISCUSSION.

#### 1.4 Overview of the research

In this work we hypothesize that the top micrometers of a hydrogel surface provide lubrication as a complex fluid domain, with rheology arising from mechanics of the solvated polymer network. Stepped, constant-velocity triborheometric measurements map the lubricating regimes between polyacrylamide and a smooth impermeable annulus over 4+ decades of slip speeds. Significant hysteresis was observed in the torque response of the interface under a light

applied pressure as sliding speed was systematically stepped in both increasing and decreasing directions. Further, we identify 3 distinct lubricating regimes based on transient and steady-state torque response. This new perspective contextualizes surfaces with complex solvated components in terms of their time-dependent rheological behavior, which directs tribological performance. Finally, it further supports a combined rheology/tribology approach for the lubrication in complex soft interfaces.

1.5 Figures

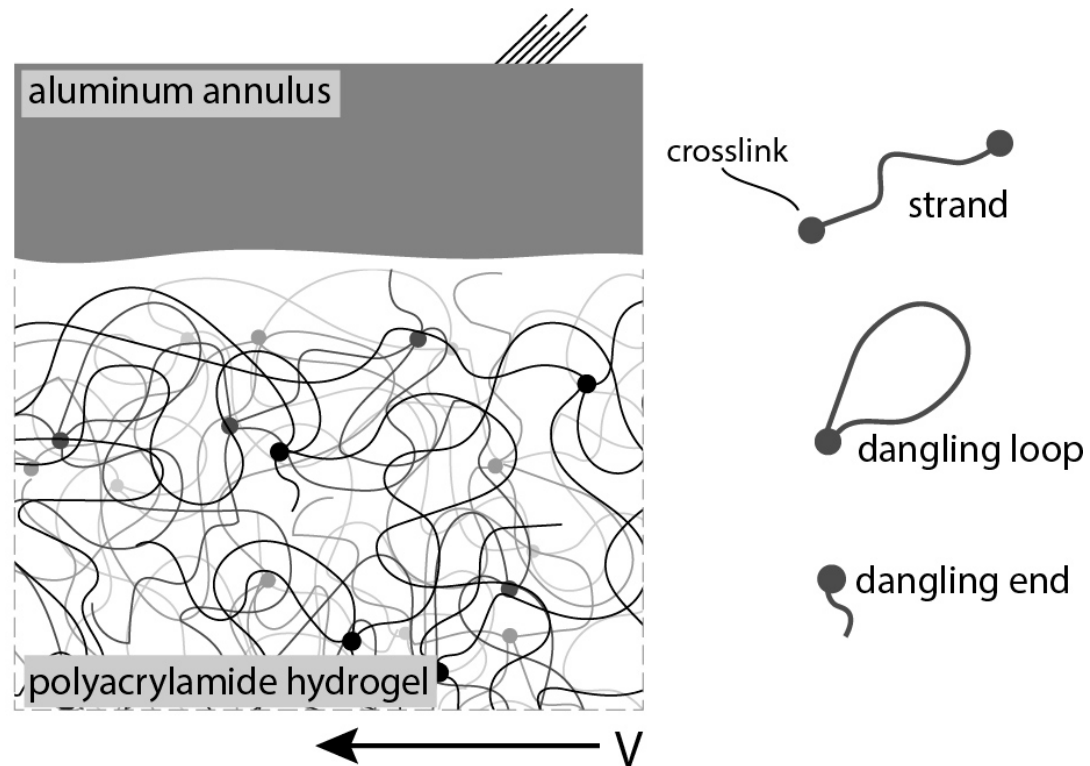


Figure 1.1 Multiple morphologies of polymer chains in a polyacrylamide hydrogel surface such as strands, dangling loops, and dangling ends

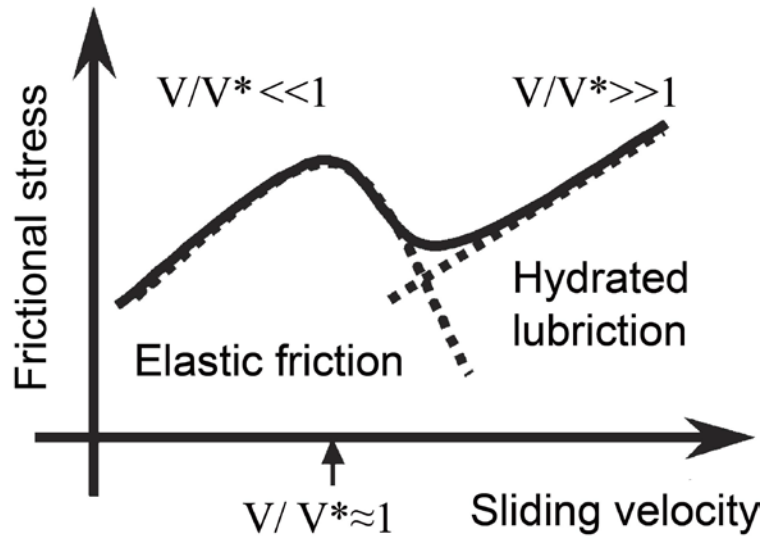


Figure 1.2 Adhesive case of “repulsion-adsorption model” [1]

### Gemini Hydrogel Surfaces

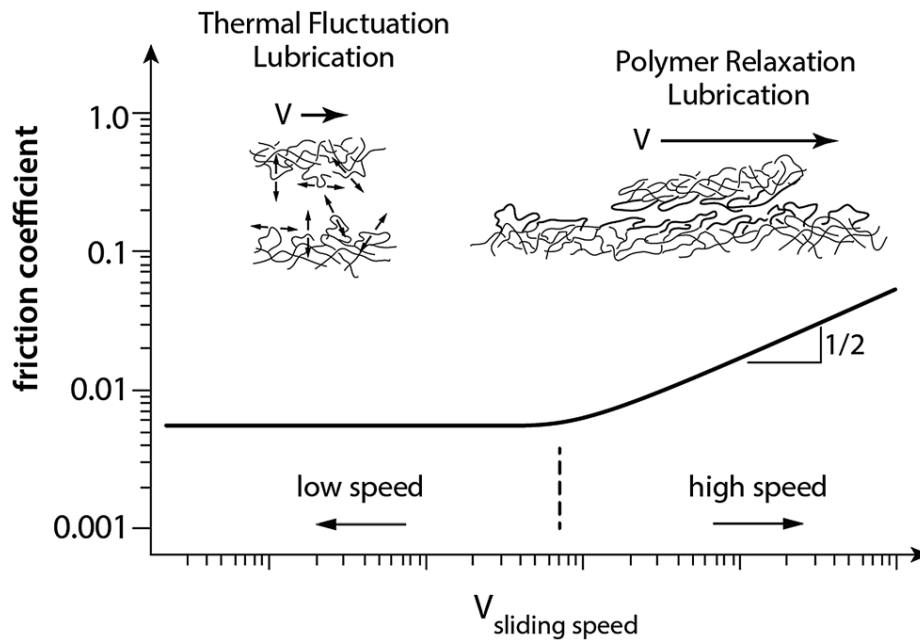


Figure 1.3 “Gemini hydrogel lubrication model” [2]

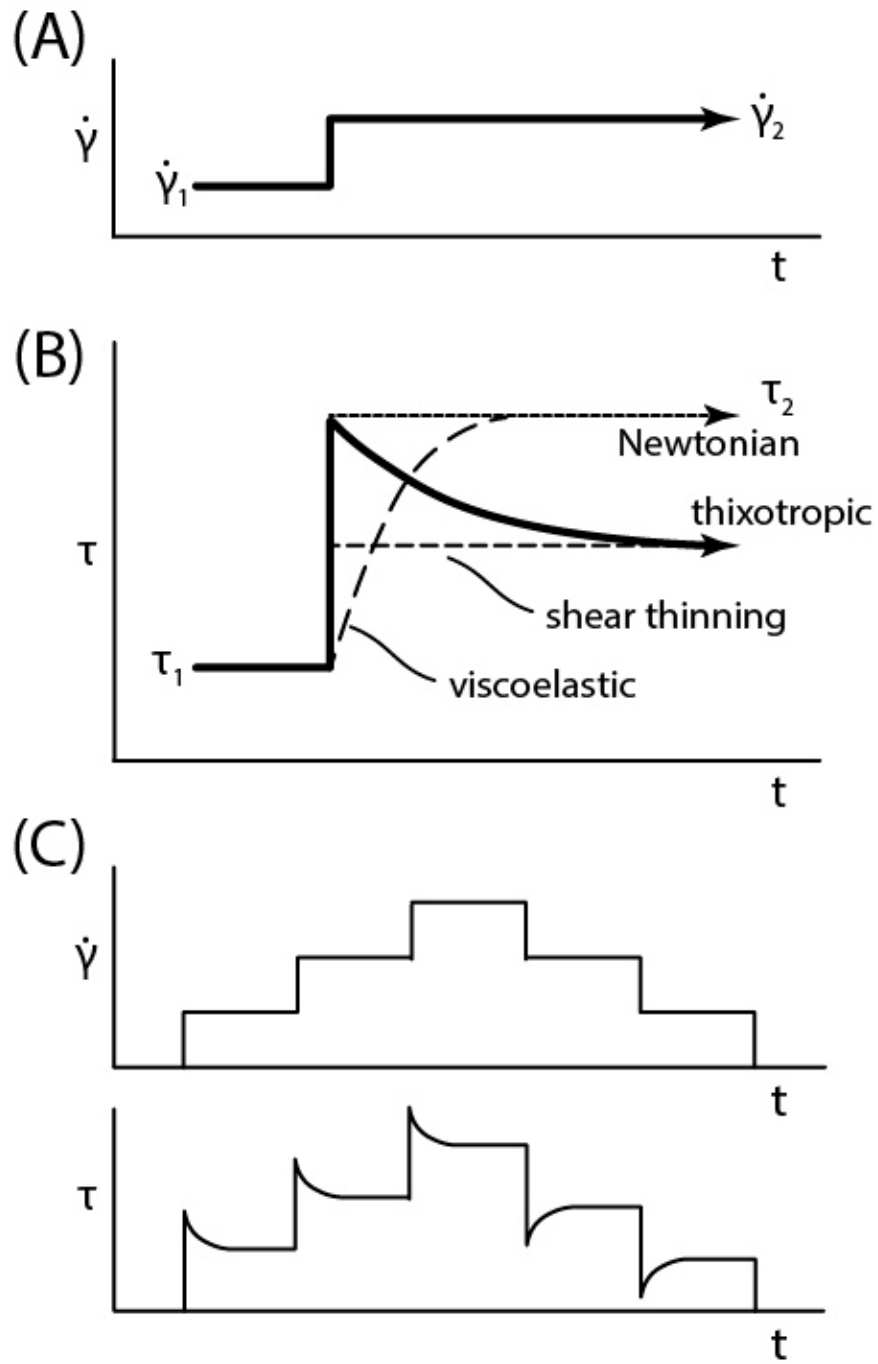


Figure 1.4 Characteristic of thixotropic fluid. Adapted from Mewis et al [28]



## CHAPTER 2: MATERIALS AND METHODS

Lubrication is typically studied with tribometers, but can be studied in any interface where slip can be prescribed

### 2.1 Experimental setup and materials

In the present work, we utilize a rotational combined-motor-transducer rheometer (DHR-3, TA Instruments, New Castle, DE USA) to prescribe constant-shear sliding, described in literature as tribo-rheometry [23], [24]. An aluminum annular geometry with 40-mm outer diameter, 36-mm inner diameter, and RMS roughness of  $R_q = 7$  nm was used as the counter-surface for the hydrogel. Parallel plate rheometers with radially-varying shear rates can be re-fitted with the aluminum annulus to provide a sliding interface with annular contact area that experiences an effectively uniform slip velocity, which allows identification of transitions in the lubrication regime that depend upon sliding speed. (Figure 2.1). The attachment and alignment of geometry on the rheometer plate is described in Figure 2.2.

A circular slab of 7.5% polyacrylamide was used as a counter surface for the aluminum annulus. The upper surface of the hydrogel slab was molded under a flat polystyrene plate. The composition of polyacrylamide is shown in Table 2.1.

## 2.2 Experimental conditions

The tribo-rheometric torque response between the aluminum ring fixture and the hydrogel slab was measured during step changes in angular velocity between  $\omega=0.05$  rad/s and 50 rad/s. Before rotation, aluminum-hydrogel contact was established by applying a normal load of  $F_N \sim 1.0$  N through decreasing gap height; gap height remained fixed during rotation. Step changes were systematically prescribed at 15 levels starting from the lowest speed and increasing to the highest, with a hold time of between  $t=60$  and 90 seconds to reach steady-state torque. The experiment was not stopped at the highest speed, but rather stepped back down symmetrically. Instantaneous torque and steady-state torque were recorded at each velocity. Because hydrated polymer mesh mechanics rely on thermal temperature, a further experiment was conducted by repeating this procedure at 3 temperatures (5, 15, and 25°C) controlled by a Peltier plate below the hydrogel sample dish. The setup was allowed to come to temperature over  $\sim 60$  minutes prior to testing.

## 2.3 Figures

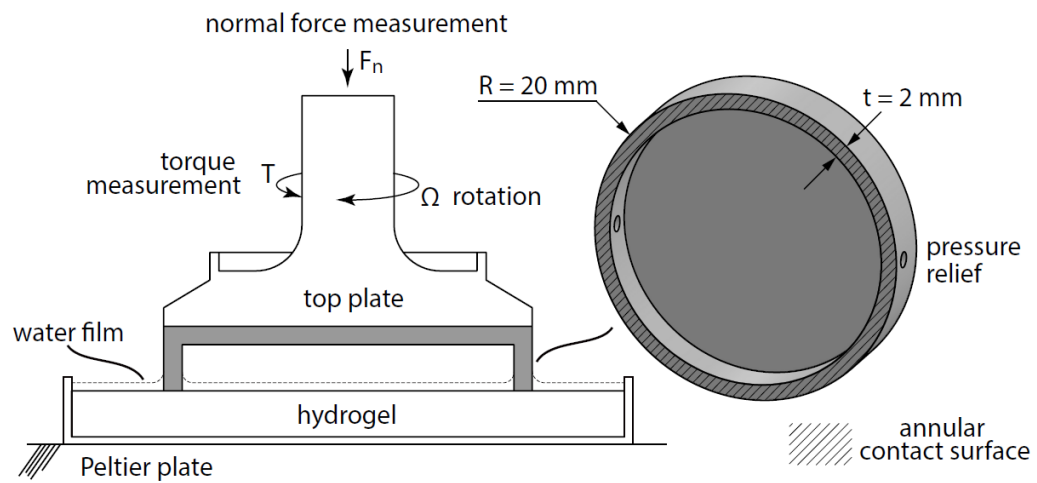


Figure 2.1 Experimental setup

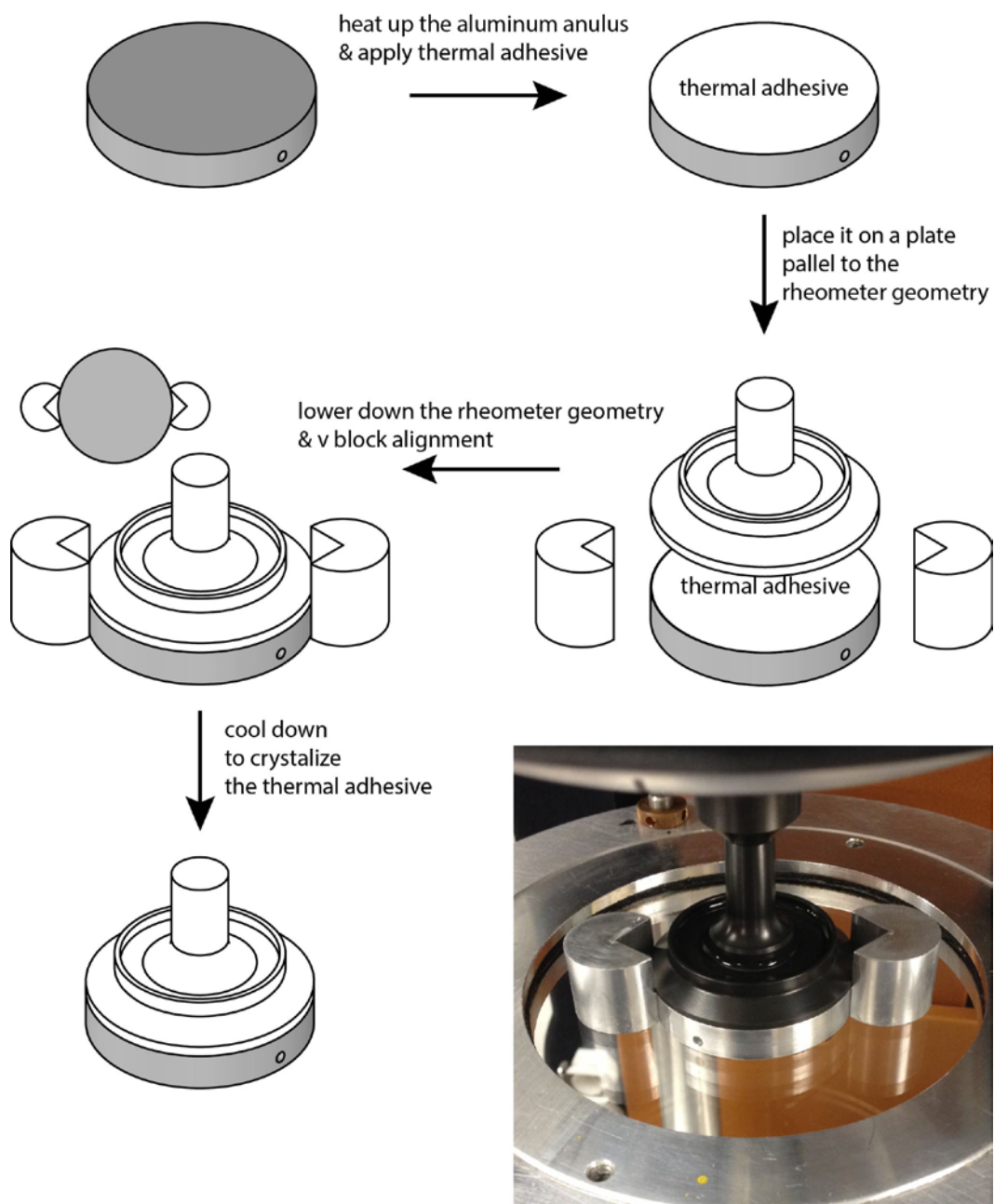


Figure 2.2 Attachment & alignment of the aluminum geometry

## 2.4 Tables

Table 2.1 Composition of hydrogel slabs molded for tribo-rheometry measurements.

Polyacrylamide hydrogel composition by mass		
acrylamide (AAm)	monomer	7.5%
N,N'-methylenebisacrylamide (MBAm)	crosslinker	0.3%
ammonium persulfate (APS)	radical initiator	0.15%
N,N,N',N'-tetramethylethylenediamine (TEMED)	catalyst	0.15%
deionized water	solvent	~92%

## CHAPTER 3: RESULTS

### 3.1 Lubrication curves for soft hydrated interfaces.

The first result from this work is that a distinct intermediate lubrication regime, characterized by duration-dependent torque response, emerged between the previously described regimes at low- and high-speed sliding. This result arose from careful examination of the instantaneous versus steady-state torque responses during a stepped velocity experiment that spanned multiple lubrication regimes.

After the aluminum ring was loaded against the hydrogel to  $F_n \sim 1.0$  N (pressure  $P \sim 4.2$  kPa), a single series of stepwise increases in angular velocity was prescribed, which imparted stepwise sliding speeds to the interface (Figure 3.1A). Minimum step time duration was 60 seconds and extensions of up to 30 additional seconds occurred in the event that torque response did not reach steady state. In all cases, the steady-state torque response was recorded as the average torque response over the last 15 seconds at each speed step. At the highlighted steps ( $\omega = 0.05, 0.5, 5,$  and  $50$  rad/s), both the steady-state torque and the transition from the instantaneous torque response changed between slow, moderate, and high sliding speeds (Figure 3.1B). At slow speeds of  $\omega = 0.05$  rad/s and  $\omega = 0.5$  rad/s, corresponding to linear speeds of approximately  $v = 0.95$  mm/s and  $v = 9.5$  mm/s,

the interface responded with no time dependence, i.e. instantaneous and steady-state torques were identical, at  $T \sim 900 \mu\text{N}\cdot\text{m}$  and  $T \sim 6,000 \mu\text{N}\cdot\text{m}$ , respectively. However at  $\omega = 5 \text{ rad/s}$  ( $v = 95 \text{ mm/s}$ ), the instantaneous response was 37% higher than steady-state, dropping off with a characteristic time constant on the order of minutes. At the highest speed  $\omega = 50 \text{ rad/s}$  ( $v = 950 \text{ mm/s}$ ), the instantaneous response was 12% higher than steady-state, dropping off with a shorter characteristic time constant on the order of 10s of seconds. This indicates that during the region considered previously as a transition regime [31], the interface experienced a relaxation behavior upon application of step increases in sliding speed. The curve resulting from the steady-state response at all steps of increasing angular velocity indicates two regimes of increasing torque with speed interrupted by a regime of decreasing torque with speed (Figure 3.1C); this steady-state lubrication curve was anticipated from prior hydrogel lubrication studies[1]. The change in torque with respect to angular speed at slower speeds  $\omega < 1 \text{ rad/s}$  fit to a simple power law  $T \propto \omega^n$  indicates an exponent  $n = 0.86$ , or  $n < 1$ , indicating shear-thinning character. The increased instantaneous torque when speed is increased to steps of  $\omega = 2 \text{ rad/s}$  to  $\omega = 11 \text{ rad/s}$  demonstrates that a family of lubrication curves could be reported for a single interface based only on the duration of each velocity step, with a family of intermediate maxima and minima indicating different lubrication behavior.

### 3.2 Lubrication hysteresis.

When the step changes in angular velocity are reversed to be decreasing, the resulting curve does not follow the increasing case, but rather shifts the inflection points to occur at lower angular speeds (Figure 3.2A). In addition, the measured steady-state torque is lower at every point. The initial overshoot at each step was consistently observed to correspond to the direction of velocity changes: stepping up in speed produced higher initial torque dropping to steady state, while stepping down in speed produced a lower torque rising to steady state. This hysteresis is significant, with steady-state torque a factor of 3 lower under a decreasing speed than an increasing speed (where  $T \sim 3,500 \mu\text{N}\cdot\text{m}$  versus  $T \sim 10,500 \mu\text{N}\cdot\text{m}$ , respectively). The observed hysteresis was challenged by up to three consecutive passes of increasing and decreasing speed steps while the temperature was held constant at 15°C. Slight changes were noted between the first cycles and the remaining two cycles, though in general the measured torques were identical, and the overall hysteresis repeatable over multiple cycles (Figure 3.2B). Three distinct regimes emerged, labeled as (1)-(3) for steps of increasing velocity, and (1')-(3') for steps of decreasing velocity, for the sake of distinguishing them for discussion.

### 3.3 Induced Normal Stress.

Rheology experiments were gap-controlled rather than normal force-controlled, so any variation in normal force arose from the dynamic behavior of the slip



interface. Up to 10% change occurred in normal force over the 4+ decades of slip speed change (Figure 3.2C). Though the change is small compared to the order-of-magnitude change in the torque over the same region, both the torque and normal force change in parallel at the same velocity steps, and therefore the induced normal force contributes to the identification of lubricating mechanisms. On steps of increasing slip velocity in the low-speed region (1), the normal force decreases slightly. As the torque moves through the maximum, a normal force is simultaneously induced (2), and continues to rise for the remainder of the increasing speed steps, (3). Finally, the induced normal force drops monotonically with steps of decreasing speed, though does not always return to the original value.

#### 3.4 Temperature inquiry.

The ability of temperature to affect the lubrication behavior was investigated by conducting three consecutive cycles of increasing and decreasing speed steps while the temperature of the hydrogel side was held constant at 5°C, 15°C, and 25°C using a Peltier plate (Figure 2.1). No significant effects were observed, though there were two minor effects: the first, higher temperatures resulted in slightly lower measured torque, especially at moderate and fast speeds; the second, higher temperatures tended to shift the duration-dependent lubrication regime, labeled regions (2) and (2') in Figure 3.2B, to slightly higher speeds, especially for steps of decreasing sliding speed (Figure 3.3).

### 3.5 Figures

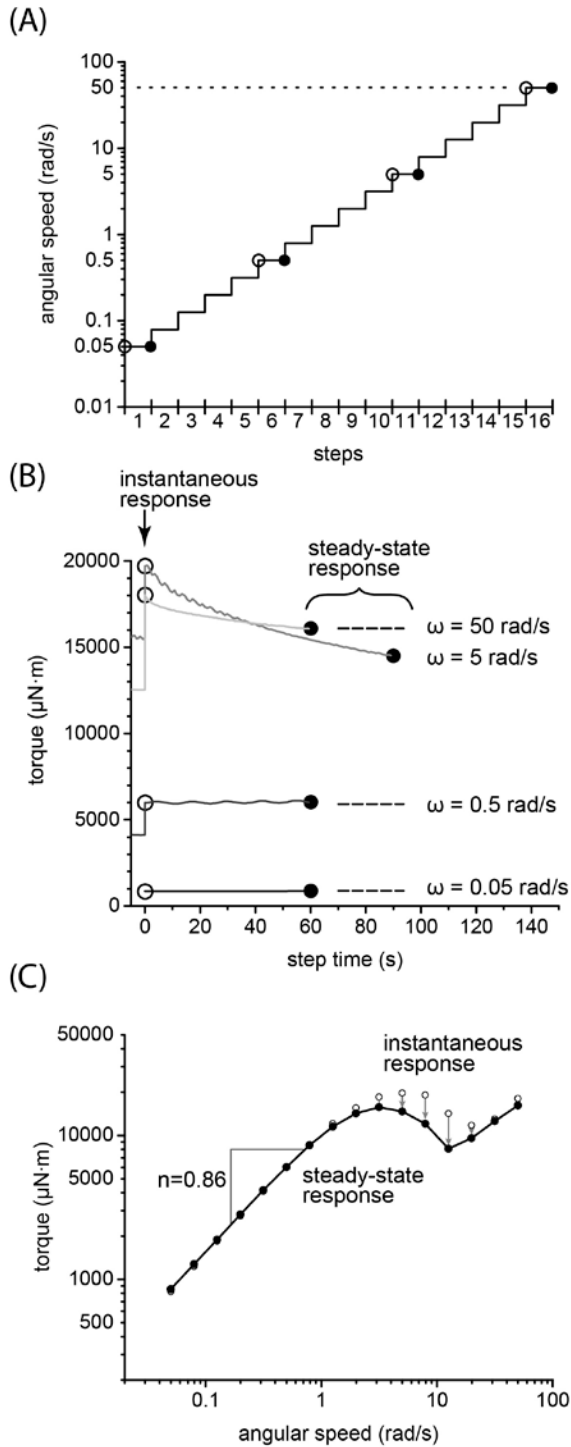


Figure 3.1 Torque responses under step increase of angular speed.

(A) 15 increasing step-changes in angular speed between 0.05 rad/s and 50 rad/s.

(B) The torque responses at step 1, 6, 11, and 16, where angular speeds are 0.05, 0.5, 5, and 50 rad/s respectively.

(C) Instantaneous ( $\circ$ ) and steady-state responses ( $\bullet$ ) plot. The biggest difference appears at moderate speeds.

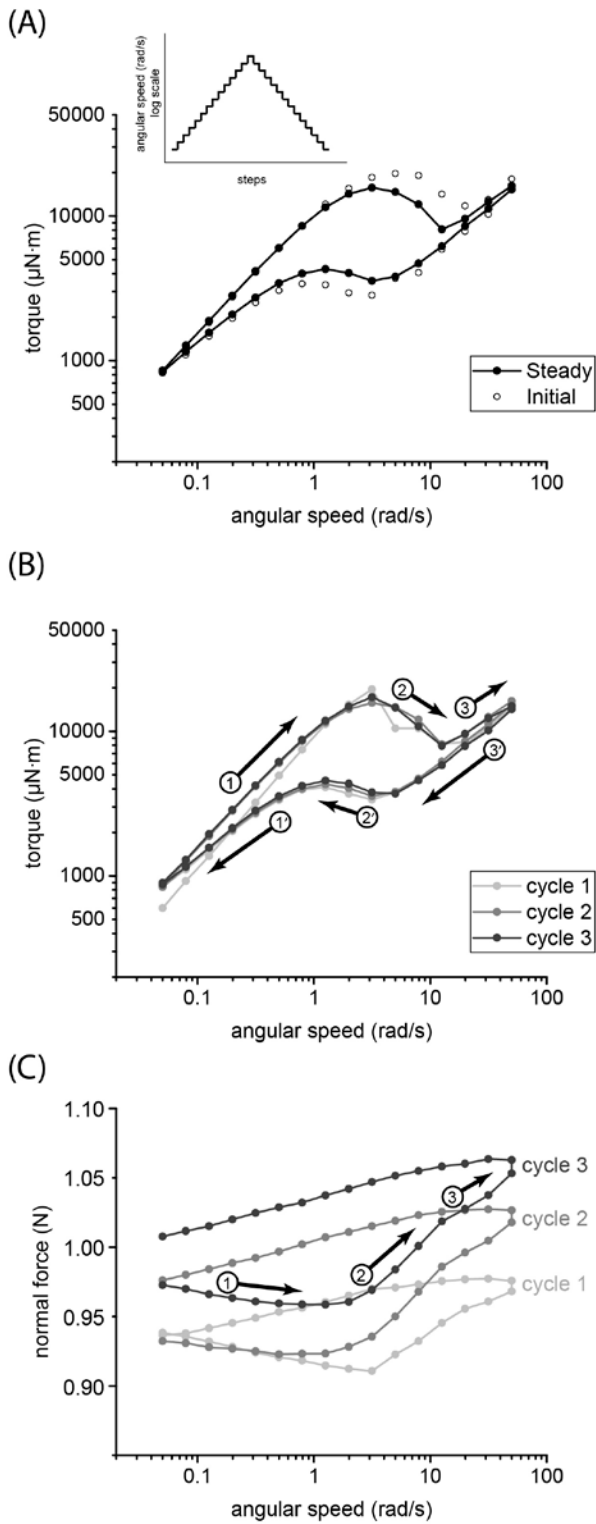


Figure 3.2 Torque responses under a full cycle of step increase-decrease in sliding speed.

(A) Instantaneous ( $\circ$ ) and steady-state responses ( $\bullet$ ) plot in a full cycle of step change in angular speed. It shows a significant hysteresis.

(B) Steady state torque response plots of consecutive 3 cycles of angular speed step change. Repeatability is shown after the first cycle.

(C) Induced normal force.

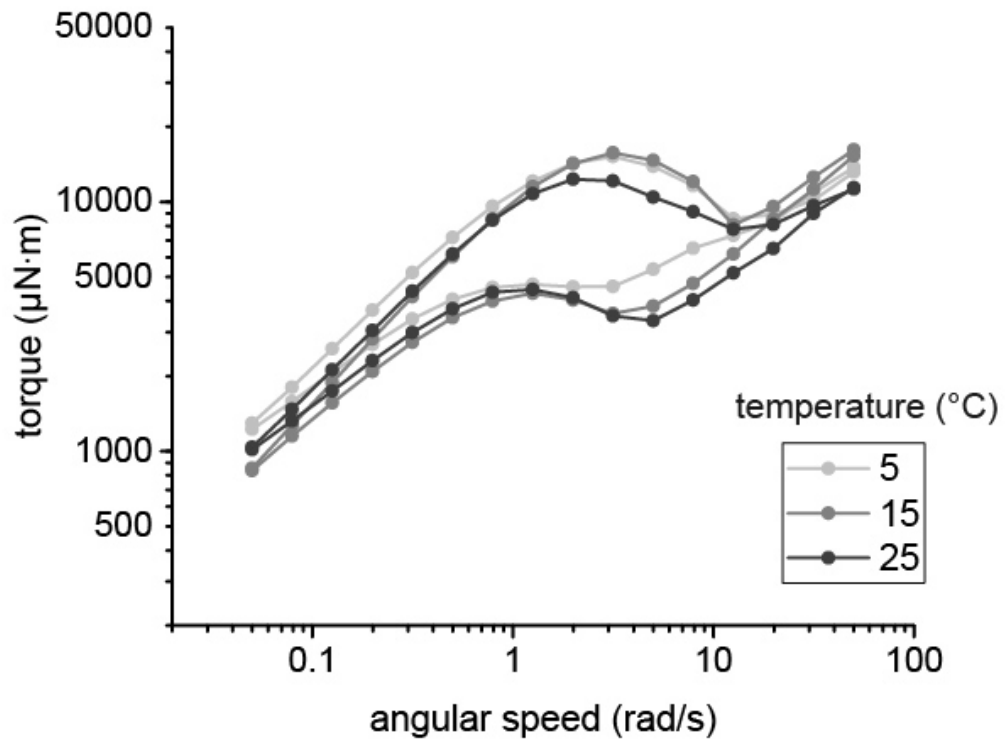


Figure 3.3 Temperature dependence of torque response. This plot compares the second full cycle of increasing and decreasing step speeds in 3 separate experiments in which the hydrogel sample was cooled to 5°, 15°, and 25°C through the Peltier stage.

## CHAPTER 4: DISCUSSION

### 4.1 Tribology of Soft Hydrated Interfaces.

#### 4.1.1 Friction Models.

Modeling the friction of soft hydrated interfaces, and specifically for hydrogel surfaces, has stemmed from rubber elasticity [1], polymer physics [16], and biphasic materials theories [32]. In particular Shallamach rubber elasticity theories were the basis for pioneering work in hydrogel lubrication, differentiated based on the adhesive or repulsive properties of hydrogel surfaces to their countersurface and later incorporating the concept of a relaxation velocity that competes with single chain relaxation timescales [33], [34]. The shape of the lubrication curve obtained using stepwise increases in angular velocity aligns well with the adhesive case model of friction according to these studies, which is based on the intermittent making and breaking of adhesive connections between the polymer phase of the hydrogel surface and the solid countersurface over a surface area that is very large compared to the size of any given adhesive event. At faster speeds there is hypothesized to be a transition characterized by a decrease in torque as fewer adhesive events are able to occur, finally reaching hydrodynamic-like lubrication at very high speeds where lubrication behavior is dominated by the viscous shear of a fluid layer rather than adhesive effects.

However, the dramatic hysteresis observed in the present work is not fully explained by the adhesive case of the repulsion-adsorption model because it assumes symmetry in increasing and decreasing speeds, a *duration-independent mechanism*.

Moreover, the relaxation time for a single chain is inversely proportional to the free energy and directly proportional to the viscosity of the solute – in this case water (Eqn 1.2). For an increase in temperature from 5°C to 25°C (278K to 298K), the relaxation time is expected to decrease by the ratio of absolute temperatures,  $\tau_{25}/\tau_5 \propto T_5/T_{25} = 0.933$ . However, the relaxation time is also expected to decrease by the ratio of water viscosities at those temperatures  $\tau_5/\tau_{25} \propto \eta_{25}/\eta_5 = 0.588$ . Assuming the mesh size is constant, the relaxation time should decrease by  $\tau_5/\tau_{25} = 0.549$ , dominated by the water viscosity changes. Prior hypotheses place the transition points in tribo-rheometric lubrication to be at the speed where the time to traverse a single mesh size (Eqn 1.1), is surpassed by the polymer relaxation time [1]. If this is the case, the local maximum on the  $T$  vs  $\omega$  plot between duration-independent and strongly duration-dependent regimes would be anticipated to increase by a factor of  $V^*_{25}/V^*_5 = 1.821$  with a change in temperature of 20 degrees. The present experiments find no trend of the threshold velocity  $V^*$ .

In addition, the model predicts one local maximum for a single temperature, but we observe two: one while increasing speed and another while decreasing speed.

This mismatch further lends support to the hypothesis that the observed hysteresis is due to a complex fluid of morphologies that cannot be described as a single chain with length equal to the mesh size, but rather is the combined effect of multiple unknown polymer terminations.

Very recent work has considered a biphasic model for lubrication in cartilage interfaces, in which the contact modulus as measured at the surface, or the contact modulus, at instantaneous and extended time points which correspond to cases of fluid support and fluid squeeze-out, respectively [35]. Though cartilage may be less permeable than 7.5 weight percent polyacrylamide hydrogel ( $k=6 \times 10^{-4} \text{ mm}^4 \text{ N}^{-1} \text{ s}^{-1}$  versus  $k=3 \times 10^{-3} \text{ mm}^4 \text{ N}^{-1} \text{ s}^{-1}$ , respectively [32], [36]), cartilage components provide other osmotic driving forces which make it a good candidate for biphasic lubrication. The present work limits applied pressure to a very low value  $< 5 \text{ kPa}$  over a annulus of contact defined by ring width of  $w=2 \text{ mm}$ , predicting a time of order  $10^9$  seconds in order to cause pressure-driven flow. The experiments described here last  $\sim 135$  minutes, so in general they are unaffected by poroelastic relaxation. The repeatability of torque response indicates that long-time effects are minimized (Figure 3.2B).

Friction coefficient is a single parameter describing a complex system of materials, surface features, fluids, and running conditions, so we do not yet have a quantitative prediction for friction coefficients in these systems. According to the simple procedures outlined by Kavehpour & McKinley for converting torque to

friction coefficient [23], our experiments have friction coefficients  $\mu=0.04$  to  $0.9$ . While this appears to be high for a compliant hydrated system, friction coefficient of  $\mu>0.3$  have been reported prior when the contact area is stationary on the hydrogel, with continued local dehydration over many cycles [37].

#### 4.1.2 Surface stability under shear.

Energy-dissipating friction mechanisms can sometimes be attributed to permanent surface changes and wear, especially for bulk polymers with high mobility such as polytetrafluoroethylene (PTFE) tribology [38]. However, our aqueous hydrogel/aluminum interface likely lacks the surface energies necessary to extract individual chains; because of this, no permanent deformation or wear was predicted. No gross wear debris was observed; however, due to the small local nature of the contact, mechanical characterization following lubrication experiments may reveal changes, and is reserved for future investigations.

#### 4.1.3 Anchored Complex fluid lubrication.

The surface termination of submerged hydrogels is not well characterized, but likely has some concentration of chain ends and loops that extend into solution; this means that the boundary between hydrogel and supernatant fluid has a concentration gradient. Solvated species in a shear flow find a large body of literature in complex fluids, where the aggregate mechanics of a fluid comprised



of various materials and structures is studied by applying a known strain and measuring the stress response. Traditionally, tribology has made use of rheological properties, but mostly in service of understanding the changes in viscosity that may help or hinder lubrication, such as promoting elastohydrodynamic lubrication. However, we use rheological measurements in order to understand the time-dependent tribological response of a hydrogel-aluminum interface.

The strong duration-dependent lubricating regime between two less duration-dependent regimes indicates that components restructure in time, and that morphologies are affected by the conformation of their neighbors (chain-chain interactions). In general this duration-dependent response is termed “thixotropy,” in which the effective viscosity decreases over time by the action of flow, and is recovered when the flow slows.

The distinct lubrication regimes can be further identified using an overlay of the instantaneous response (Figure 3.1B) following every step change in velocity, presented in Figure 4.1. Since step time varies between 60 and 90 seconds, the horizontal axis of each step curve is normalized by its step time (Figure 4.1 inset). The normalized step curves are placed at corresponding steady state points to show the converging trend of torque value at each point. Torque values along the vertical axis for all the step curves are real torque values in log scale, identical to Figure 3.2A. At every step of increasing speed torque increases, then either

remains constant or relaxes down depending upon the speed; this is a behavior of the duration-dependent restructuring described in Figure 1.4. Similarly, at every step of decreasing speed torque decreases, then either remains constant or relaxes up to steady-state. So, we consider the duration-dependent lubrication to find its analog in thin film flow of a thixotropy-like restructuring complex fluid. That said, we struggle to define this interface in terms of rheological parameters of shear rate,  $\dot{\gamma}$ , because the effective fluid layer thickness is not well-defined. Given that the shear stress is directly proportional to the measured friction torque,  $\sigma \propto T$ , and the shear rate is directly proportional to sliding velocity,  $\dot{\gamma} \propto \omega$ , we assume that the provided  $T(\omega)$  curves have identical shape with the common  $\sigma(\dot{\gamma})$  curves.

Some complex fluids such as polymers, clay, or colloidal microgels restructure based on discrete events, such as shear banding, of the non-continuum components. These discrete events have recently started to be connected to the rheological behavior through a carefully-measured characteristic timescale,  $\theta$ , that issues from the inflection in the magnitude of rheological hysteresis over a spectrum of relaxation times,  $\delta t$ , at each constant shear rate [39]. When shear interrupts physical aging, the material structure is re-broken, leading to hysteresis depending upon increasing or decreasing shear rates. While this elegant conclusion is appealing to directly apply to a tribological system, we believe that the observed duration-dependent behavior arises from the lubricating regime in

addition to structural reorganization. A more apt description of the hydrogel-aluminum sliding interface is that it acts as a variety of complex fluids at different lubricating conditions, which is not yet experimentally explored. Thus, *rheological hysteresis* may be a basis for describing *tribological hysteresis*.

## 4.2 Conceptual complex soft interface lubrication.

### 4.2.1 Lubrication regimes.

Based on prior studies and the observed hysteresis, we postulate the following mechanistic path for a hydrogel-aluminum interface as it experiences multiple duration-dependent lubrication regimes, starting from the lowest speed and increasing (Figure 4.1).

Duration-independent lubrication regime. (region (1) of Figure 3.2) At low sliding speeds, the step change in speed resulted in a time-independent step change in torque; this torque response can be described by a power law  $T \propto \omega^n$ , with exponent  $n=0.86$ , which suggests shear-thinning fluid behavior. Given that tribological measurements require an applied pressure  $\sigma > 0$ , the resistance to flow is the response of the complex interface, where the hydrogel-aluminum interaction responds instantaneously. Because of this, surface features don't appear to be entrained, but rather elastically oriented and leading to less resistance to sliding at faster speeds.

Thixotropy-like lubrication regime. (region (2) of Figure 3.2) Following the stable low-speed regime at a threshold of  $\omega=3$  rad/s ( $V=57$  mm/s), the strongly duration-dependent torque response indicates a restructuring of the interface. Tribological Stribeck lubrication curves indicate this region of decreasing friction as “mixed lubrication” where the partial boundary contact (diminishing asperity-asperity friction) and partial fluid film (intensifying fluid shear friction) contribute to the friction response [40], though in the present work the soft nature of the interface precludes the definitions of boundary and fluid film lubrication. Because of this, we postulate that the interface *as a complex fluid* allows the interface restructuring to be the mechanism for lubrication in a broader regime than typically observed in mixed lubrication – the strongly duration-dependent lubrication with an induced normal stress (shaded in Figure 4.1). At  $\omega\sim 8$  rad/s, the torque response did not reach steady state after  $t=90$  seconds, indicating a maximum time constant for restructuring on the order of  $\tau\sim 1$  minute. This regime of decreasing torque with speed is described by a steady-state power law exponent of  $n\sim -0.87$ .

Weakly duration-dependent high-speed lubrication regime. (region (3) of Figure 3.2) The consistent slope of the increasing and decreasing lubrication curves at high speeds, along with weakly duration-dependent behavior, indicates a regime where the organization of the interface is relatively unchanging with a shear-thinning power-law exponent of  $n\sim -0.58$ . This reduction in duration dependence

indicates that restructuring of chains is limited and the lubricating behavior is more influenced by the aqueous component; this aligns strongly with Gemini hydrogel hypotheses [2]. These findings support statements regarding lack of evidence for full-film Newtonian lubrication [16], [40].

Recovery lubrication. (regions (3'), (2'), (1') of Figure 3.2) As sliding speed decreased, the same regimes appeared, though with a delayed response; the transitions to strongly duration-dependent lubrication occurred at slower speeds and lower torques, leading to the significant hysteresis. As the interface experienced decreasing speeds below  $\omega < 0.7$  rad/s, the duration dependence did not completely resolve until the lowest sliding speeds  $\omega \sim 0.05$  rad/s. The proposed mechanism of this slow return to duration-independence is based on the recovery of the surface chains from a more oriented state to less oriented state.

#### 4.2.2 Possible mechanisms for thixotropy-like lubrication

While the physics of polymer chain stretch and relaxation are likely involved, additional possible mechanisms that influence lubrication include orientation along the sliding direction (by bending and stretch), and effective stiffening of the surface. In duration-dependent bulk fluid flows, floating particles may attract each another with weak bonds, causing the formation of flocs. However, the weak bonds are easily broken by the action of flow causing breakup of the flocs into

smaller ones when the shear rate increases, and thus, fluid becomes easier to flow, or its viscosity decreases[28].

Because this work draws from polymer physics, materials science, solid mechanics, and fluid mechanics, there are multiple possible mechanisms responsible for the appearance of thixotropic-like behavior of the hydrogel-aluminum lubrication. Two are discussed below in more detail: polymer chain alignment and effective hydrodynamic pressurization.

Polymer chain alignment If we consider hydrogel lubrication as a plug flow through a sparse “forest” of surface-terminated polymer chains at the interface, the action of flow tends to entrain the chains and orient them along the sliding direction, causing less resistance to shear (Figure 4.2). Prior literature suggests similar mechanisms, though without the duration dependence specifically addressed [2], [16], [41]. Solid polymers undergoing chain alignment consider it to be a permanent deformation, or plastic deformation, whereas in this system there would likely be multiple time constants of polymer stretch and contraction based on the dynamics of a branched polymer in shear flow.

Effective hydrodynamic pressurization At moderate speeds in the regime denoted as region (2) in Figure 3.2B-C, there is a simultaneous drop in shear stress and increase in normal stress. This mimics the drop in friction coefficient on the

Stribeck curve for engineering materials, indicating partial fluid load support because the resistance to fluid shear is much lower than resistance to asperity-asperity slip.

This increased pressure may compress the polymeric component of the hydrogel surface. Compressed hydrogel would increase the effective fluid film thickness between the surfaces, and therefore, fluid becomes easier to flow. (Figure 4.3 A) We can analyze this situation with effective viscosity  $\eta^*$  by introducing apparent shear rate  $\dot{\gamma}^*$ , which uses constant film thickness in calculation for it. (Figure 4.3 B) Since Figure 4.3 A and B are describing the same torque response, or the same shear stress response, in two different ways, we can equate shear stresses in two cases and this results in effective viscosity decrease at a higher sliding speed. (Figure 4.3 C) If the deformation occurs gradually over time because of poroelastic relaxation, this can be one possible mechanism for thixotropic behavior.

However, the parallel-plates experimental setup does not overtly provide any wedge geometry to entrain or pressurize an elastohydrodynamic film. Therefore, the induced normal force may arise from deformation and orientation of surface features and/or local fluid pressurization of small interface regions due to surface roughness, rather than creation of a full fluid film.

### 4.3 Figures

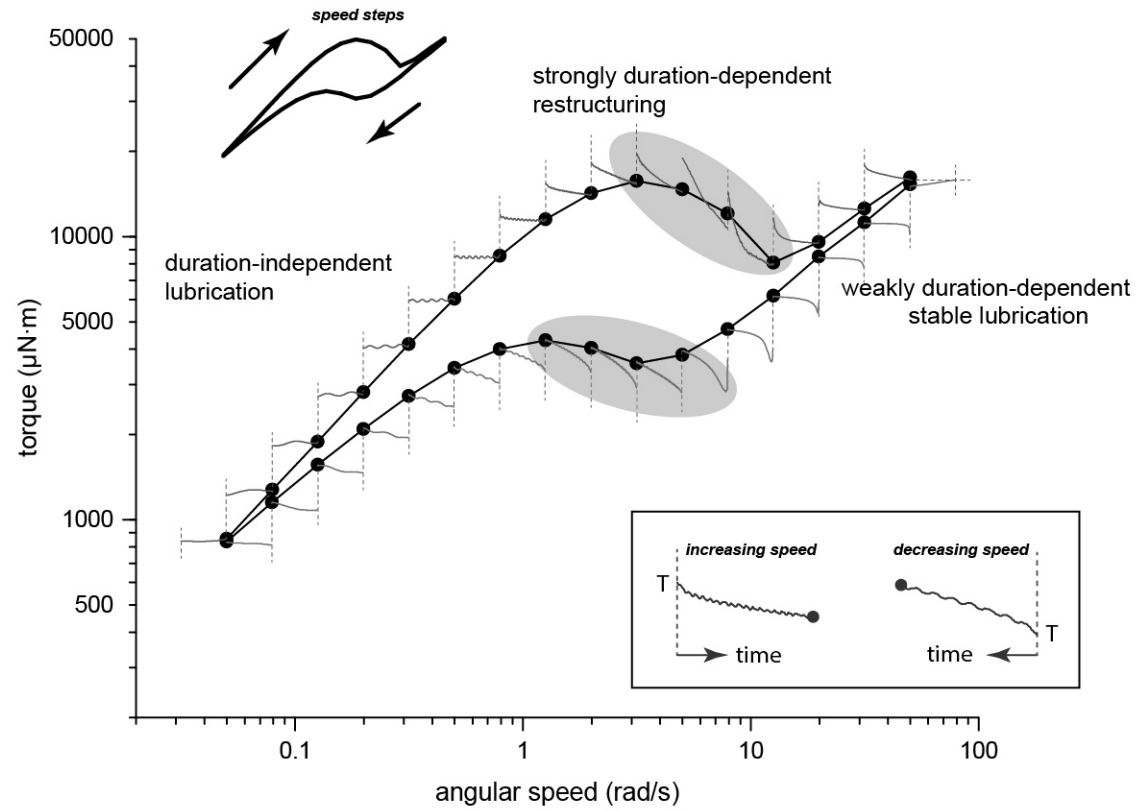


Figure 4.1 Lubrication regimes based on duration dependence of torque response.



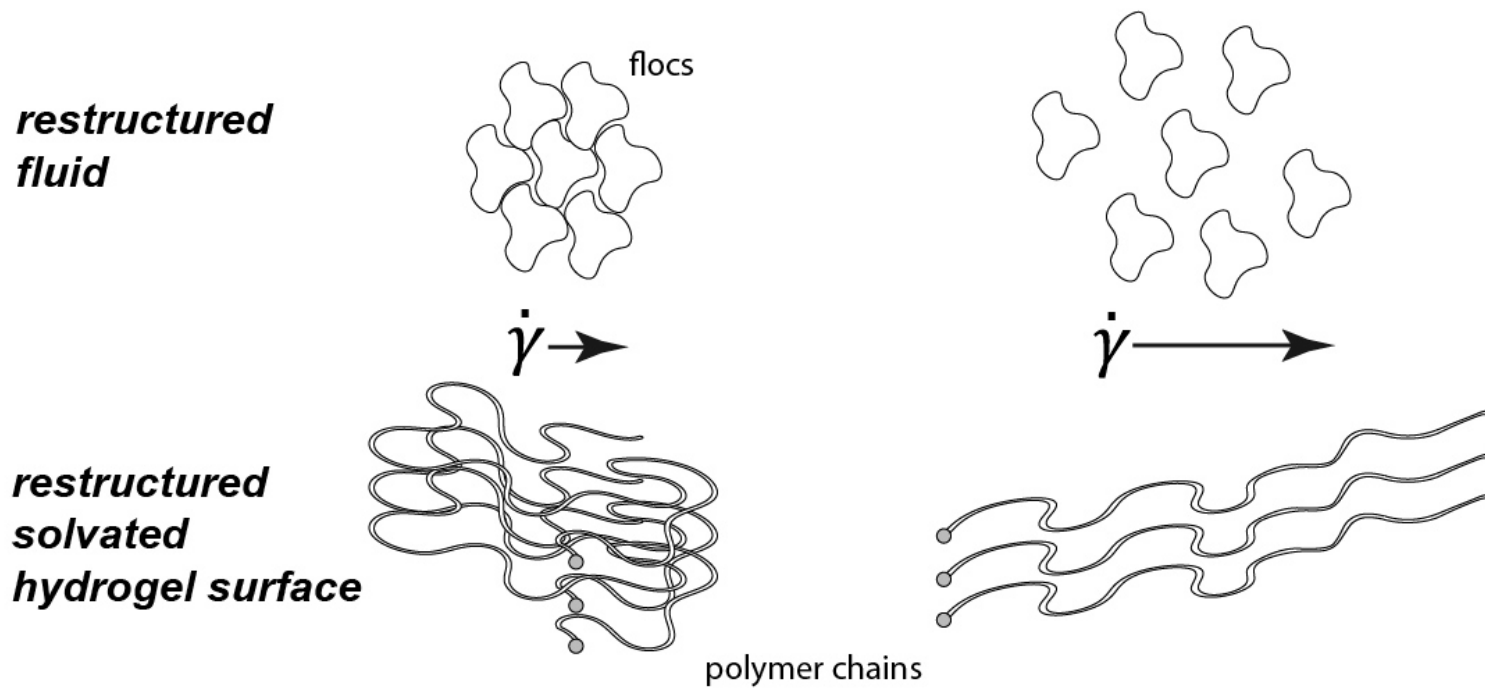


Figure 4.2 Analogy between thixotropic fluid flow and hydrogel lubrication. In the same way that the interaction of polymers or flocs in a complex fluid drives its modes of dissipation in shear flow, the entrainment of polymeric elements in a hydrogel-aluminum sliding interface may drive its lubrication response

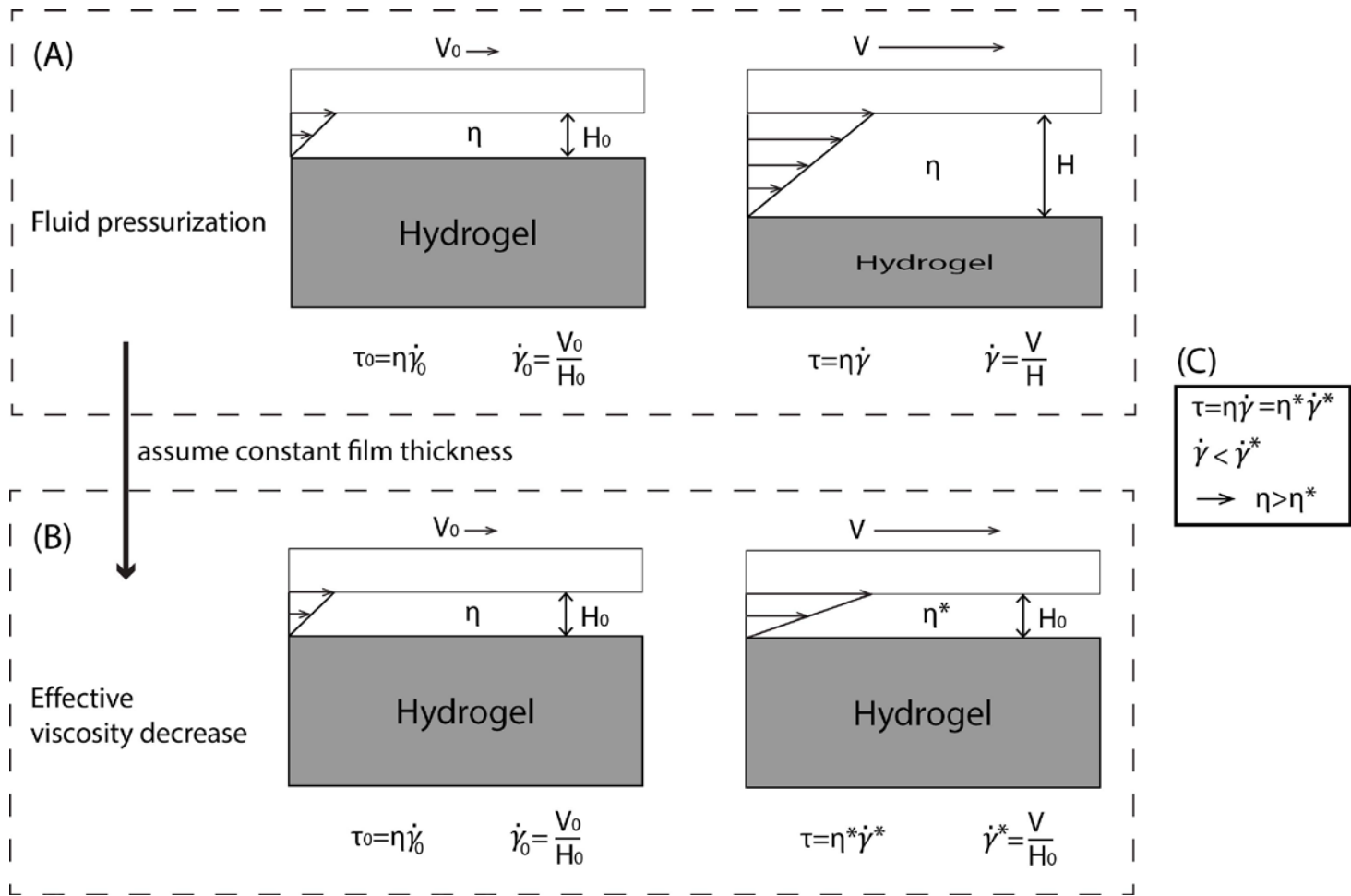


Figure 4.3 Effective viscosity decrease by the action of hydrodynamic pressurization

## CHAPTER 5: CONCLUSION

The corneal epithelium of the eye surface relies on anchored and solved mucins which are sheared tens of thousands of times per day during blinks and other slower ocular movements. As the eyelid moves down over the cornea, the lubrication by the tear film likely moves through multiple lubrication regimes [42], shearing these mucins repeatedly, all while maintaining ocular clarity for sensing and little to no perception of the movement. Nature may exploit complex fluids anchored to a surface for desired lubrication performance through shear-driven restructuring, and conversely produce symptoms when these lubricating systems break down because of mucin dysfunction such as in dry eye disease (DES) or cystic fibrosis (CF) [43], [44]. Significant open questions remain regarding the specific polymeric components that drive lubrication under multiple regimes. Uncovering the mechanisms of biological lubrication requires the combination of the rheological framework of complex fluid mechanics with the tribological approach of applied forces over well-defined slip motions.

We draw the following conclusions from this work:

- Tribo-rheometry was used to probe the lubricating behavior of an annular polyacrylamide hydrogel-aluminum interface under stepped

velocity. Duration-dependence of the torque response was negligible at slow speeds, strong at moderate speeds, and weak at the highest sliding speeds. In the very slow and fast sliding speed regimes, the torque response was reminiscent of shear-thinning fluids.

- The inherent lubricating behavior of this interface was characterized by extensive hysteresis not attributed to material wear. The combination of hysteresis with duration-dependent lubrication suggests that the interface is a complex fluid responding to shear conditions by restructuring the presenting polymeric components within the interface.

Given the effects uncovered here, many recommendations for future work arise:

- Conducting experiments with tribometer instead of rheometer should yield similar lubrication curves, though over a smaller contact area. On an instrument with markedly better force resolution (single  $\mu\text{N}$  rather than the  $\sim 1\text{N}$  sensitivity on the rheometer), the characteristics of each regime will more easily be detected. Alignment and high sliding speeds will present the biggest challenges to this change, but it is already in progress.

- The rheometer capabilities allow for a wider variety of experimental conditions to be applied, such as higher loads, starting each sliding speed from zero, and allowing more time at each speed level. Increased normal forces may uncover a maximum pressure over which the results of this thesis are valid. Starting each speed level from zero may emphasize time effects. Allowing more time at each level may uncover the final, true steady-state torque response in the highly duration-dependent regime where 1-2 torque responses were truncated before reaching steady-state.
- In order to prove the mechanism of fluid pressurization suggested in this study, we need to conduct an experiment to see whether there is change in the gap between the solid surface and the hydrogel surface, or change in effective film thickness. One possible way is using confocal microscopy with fluorescent beads inside the gel, which can visualize the deformation of gel during the pressurization.
- Molecular dynamics (MD) simulation of polymer chains on hydrogel surfaces as an extension of this study would add considerable information regarding either the molecular-scale interactions between polyacrylamide chains and an aluminum surface or the ability of polymer chains to stretch and contract under shear flow. A simulation study on fluid-polymer chain interaction by Dutta et al [45] suggests a

suitable simulation method for polymer chain alignment mechanism described in Figure 4.2. We can investigate how a fluid flow affects the orientation and stretch of polymer chains and how these changes in polymer chains affect back the fluid flow simultaneously.

## REFERENCES

- [1] J. P. Gong, “Friction and lubrication of hydrogels - its richness and complexity,” *Soft Matter*, vol. 2, no. 7, p. 544, 2006.
- [2] a. a. Pitenis, J. M. Urueña, K. D. Schulze, R. M. Nixon, a. C. Dunn, B. a. Krick, W. G. Sawyer, and T. E. Angelini, “Polymer fluctuation lubrication in hydrogel gemini interfaces,” *Soft Matter*, vol. 10, no. 44, pp. 8955–8962, 2014.
- [3] Y. Ishikawa, K. I. Hiratsuka, and T. Sasada, “Role of water in the lubrication of hydrogel,” *Wear*, vol. 261, no. 5–6, pp. 500–504, 2006.
- [4] T. Røn, I. S. Chronakis, and S. Lee, “Lubrication of soft and hard interfaces with thermo-responsive F127 hydrogel,” *Polymer (Guildf)*, vol. 55, no. 22, pp. 5708–5717, 2014.
- [5] Y. Wu, X. Pei, X. Wang, Y. Liang, W. Liu, and F. Zhou, “Biomimicking lubrication superior to fish skin using responsive hydrogels,” *NPG Asia Mater.*, vol. 6, no. 10, p. e136, 2014.
- [6] M. M. Blum and T. C. Ovaert, “A novel polyvinyl alcohol hydrogel functionalized with organic boundary lubricant for use as low-friction cartilage substitute: Synthesis, physical/chemical, mechanical, and friction characterization,” *J. Biomed. Mater. Res. - Part B Appl. Biomater.*, vol. 100 B, no. 7, pp. 1755–1763, 2012.

- [7] T. A. E. Ahmed, E. V. Dare, and M. Hincke, "Fibrin a versatile scaffold for tissue engineering.pdf," *Tissue Eng. Part B Rev.*, vol. 14, no. 2, pp. 199–215, 2008.
- [8] M. M. Blum and T. C. Ovaert, "Low friction hydrogel for articular cartilage repair: evaluation of mechanical and tribological properties in comparison with natural cartilage tissue.," *Mater. Sci. Eng. C. Mater. Biol. Appl.*, vol. 33, no. 7, pp. 4377–83, 2013.
- [9] I. L. Kim, R. L. Mauck, and J. a. Burdick, "Hydrogel design for cartilage tissue engineering: A case study with hyaluronic acid," *Biomaterials*, vol. 32, no. 34, pp. 8771–8782, 2011.
- [10] K. L. Spiller, S. A. Maher, and A. M. Lowman, "Hydrogels for the Repair of Articular Cartilage Defects," *Tissue Eng. Part B Rev.*, vol. 17, no. 4, pp. 281–299, 2011.
- [11] R. a a Muzzarelli, "Chitins and chitosans for the repair of wounded skin, nerve, cartilage and bone," *Carbohydr. Polym.*, vol. 76, no. 2, pp. 167–182, 2009.
- [12] M. Peng, J. Ping Gong, and Y. Osada, "Substrate effect on the formation of hydrogels with heterogeneous network structure.," *Chem. Rec.*, vol. 3, no. 1, pp. 40–50, 2003.
- [13] T. Tominaga, N. Takedomi, H. Biederman, H. Furukawa, Y. Osada, and J. P. Gong, "Effect of substrate adhesion and hydrophobicity on hydrogel friction," *Soft Matter*, vol. 4, no. 5, p. 1033, 2008.



- [14] G. Sudre, D. Hourdet, F. Cousin, C. Creton, and Y. Tran, "Structure of surfaces and interfaces of poly(N,N-dimethylacrylamide) hydrogels," *Langmuir*, vol. 28, no. 33, pp. 12282–12287, 2012.
- [15] M. Rubinstein and R. H. Colby, "Networks and gels," in *Polymer Physics*, Oxford University Press, 2003, pp. 253–277.
- [16] J. M. Urueña, A. a. Pitenis, R. M. Nixon, K. D. Schulze, T. E. Angelini, and W. Gregory Sawyer, "Mesh Size Control of Polymer Fluctuation Lubrication Mechanisms in Gemini Hydrogels," *Biotribology*, vol. 1–2, pp. 24–29, 2015.
- [17] J. Choi, H. J. Kung, C. E. MacIas, and O. K. Muratoglu, "Highly lubricious poly(vinyl alcohol)-poly(acrylic acid) hydrogels," *J. Biomed. Mater. Res. - Part B Appl. Biomater.*, vol. 100 B, no. 2, pp. 524–532, 2012.
- [18] P. C. Nalam, J. N. Clasohm, A. Mashaghi, and N. D. Spencer, "Macrotribological studies of poly(L-lysine)-graft-Poly(ethylene glycol) in aqueous glycerol mixtures," *Tribol. Lett.*, vol. 37, no. 3, pp. 541–552, 2010.
- [19] A. C. Rennie, P. L. Dickrell, and W. G. Sawyer, "Friction coefficient of soft contact lenses: measurements and modeling," *Tribol. Lett.*, vol. 18, no. 4, pp. 499–504, 2005.
- [20] M. Roba, E. G. Duncan, G. a. Hill, N. D. Spencer, and S. G. P. Tosatti, "Friction measurements on contact lenses in their operating environment," *Tribol. Lett.*, vol. 44, no. 3, pp. 387–397, 2011.

- [21] E. D. Bonnevie, V. J. Baro, L. Wang, and D. L. Burris, "In situ studies of cartilage microtribology: Roles of speed and contact area," *Tribol. Lett.*, vol. 41, no. 1, pp. 83–95, 2011.
- [22] C. M. Elkins, Q. M. Qi, and G. G. Fuller, "Corneal Cell Adhesion to Contact Lens Hydrogel Materials Enhanced via Tear Film Protein Deposition," *PLoS One*, vol. 9, no. 8, pp. 1–9, 2014.
- [23] H. P. Kavehpour and G. H. McKinley, "Tribo-rheometry: From gap-dependent rheology to tribology," *Tribol. Lett.*, vol. 17, no. 2, pp. 327–335, 2004.
- [24] C. Clasen, H. P. Kavehpour, and G. H. McKinley, "Bridging Tribology and Microrheology of Thin Films," *Appl. Rheol.*, vol. 20, no. 4, pp. 1–13, 2010.
- [25] G. Kagata, J. P. Gong, and Y. Osada, "Friction of gels. 6. Effects of sliding velocity and viscoelastic responses of the network," *J. Phys. Chem. B*, vol. 106, no. 18, pp. 4596–4601, 2002.
- [26] A. Schallamach, "A theory of dynamic rubber friction," *Rubber Chem. Technol.*, vol. 39, no. 2, pp. 320–327, 1966.
- [27] S. H. Kim, A. Opdahl, C. Marmo, and G. a. Somorjai, "AFM and SFG studies of pHEMA-based hydrogel contact lens surfaces in saline solution: Adhesion, friction, and the presence of non-crosslinked polymer chains at the surface," *Biomaterials*, vol. 23, no. 7, pp. 1657–1666, 2002.
- [28] J. Mewis and N. J. Wagner, "Thixotropy," *Adv. Colloid Interface Sci.*, vol. 147–148, pp. 214–227, 2009.

- [29] C. a. Grattoni, H. H. Al-Sharji, C. Yang, A. H. Muggeridge, and R. W. Zimmerman, "Rheology and Permeability of Crosslinked Polyacrylamide Gel.," *J. Colloid Interface Sci.*, vol. 240, no. 2, pp. 601–607, 2001.
- [30] D. Calvet, J. Y. Wong, and S. Giasson, "Rheological monitoring of polyacrylamide gelation: Importance of cross-link density and temperature," *Macromolecules*, vol. 37, no. 20, pp. 7762–7771, 2004.
- [31] T. Kurokawa, T. Tominaga, Y. Katsuyama, R. Kuwabara, H. Furukawa, Y. Osada, and J. P. Gong, "Elastic-hydrodynamic transition of gel friction," *Langmuir*, vol. 21, no. 20, pp. 8643–8648, 2005.
- [32] E. D. Bonnevie, V. J. Baro, L. Wang, and D. L. Burris, "Fluid load support during localized indentation of cartilage with a spherical probe," *J. Biomech.*, vol. 45, no. 6, pp. 1036–1041, 2012.
- [33] J. Gong and Y. Osada, "Gel friction: A model based on surface repulsion and adsorption," *J. Chem. Phys.*, vol. 109, no. 18, pp. 8062–8068, 1998.
- [34] P.-G. de Gennes, *Scaling Concepts in Polymer Physics*. Ithaca, NY: Cornell University Press, 1979.
- [35] A. C. Moore, B. K. Zimmerman, X. Chen, X. L. Lu, and D. L. Burris, "Experimental characterization of biphasic materials using rate-controlled Hertzian indentation," *Tribol. Int.*, vol. 89, pp. 2–8, 2015.
- [36] M. L. Oyen, "Mechanical characterisation of hydrogel materials," *Int. Mater. Rev.*, vol. 59, no. 1, pp. 44–59, 2014.

- [37] A. C. Dunn, W. G. Sawyer, and T. E. Angelini, "Gemini Interfaces in Aqueous Lubrication with Hydrogels," *Tribol. Lett.*, pp. 1–8, 2014.
- [38] K. L. Harris, A. a. Pitenis, W. G. Sawyer, B. a. Krick, G. S. Blackman, D. J. Kasprzak, and C. P. Junk, "PTFE Tribology and the Role of Mechanochemistry in the Development of Protective Surface Films," *Macromolecules*, p. 150526153713007, 2015.
- [39] T. Divoux, V. Grenard, and S. Manneville, "Rheological hysteresis in soft glassy materials," *Phys. Rev. Lett.*, vol. 110, no. 1, pp. 1–5, 2013.
- [40] G. Stachowiak and A. W. Batchelor, "Hydrodynamic Lubrication," in *Engineering Tribology*, 4th Editio., Elsevier, 2005, p. 238.
- [41] A. C. Dunn, A. A. Pitenis, J. M. Uruena, K. D. Schulze, T. E. Angelini, and W. G. Sawyer, "Kinetics of aqueous lubrication in the hydrophilic hydrogel Gemini interface," *Proc. Inst. Mech. Eng. Part H J. Eng. Med.*, vol. 229, no. 12, pp. 889–894, 2015.
- [42] A. C. Dunn, J. A. Tichy, and J. M. Uruena, "Lubrication regimes in contact lens wear during a blink," vol. 63, pp. 45–50, 2013.
- [43] P. Ramamoorthy and J. J. Nichols, "Mucins in contact lens wear and dry eye conditions.," *Optom. Vis. Sci.*, vol. 85, no. 8, pp. 631–642, 2008.
- [44] S. M. Kreda, C. W. Davis, and M. C. Rose, "CFTR, mucins, and mucus obstruction in cystic fibrosis.," *Cold Spring Harb. Perspect. Med.*, vol. 2, no. 9, p. a009589, 2012.

- [45] S. Dutta, K. D. Dorfman, and S. Kumar, “Shear-Induced Desorption of Isolated Polymer Molecules from a Planar Wall,” *ACS Macro Lett.*, vol. 4, no. 3, pp. 271–274, 2015.

APPENDIX A

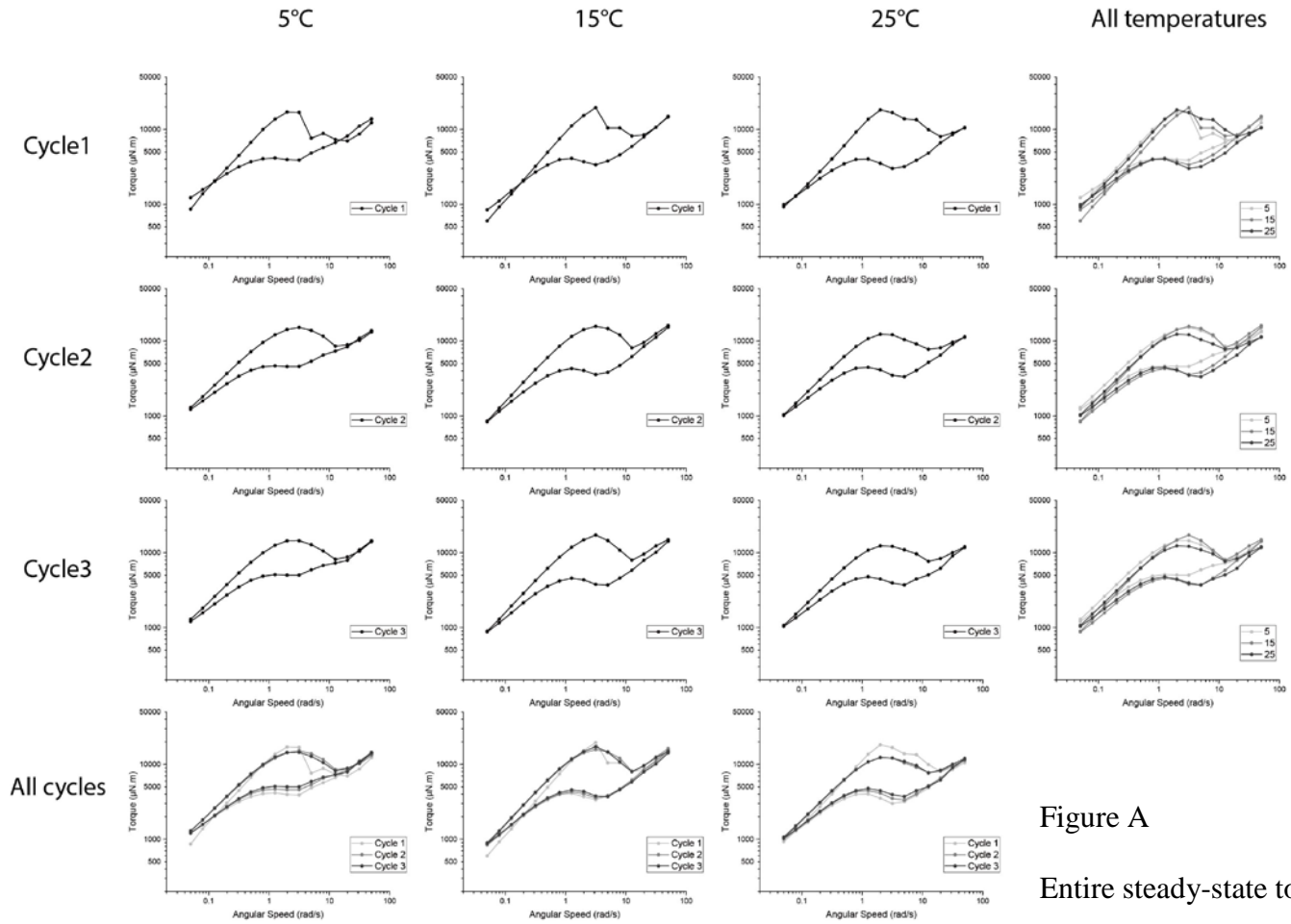


Figure A

Entire steady-state torque results